the plant journal

SEB Society for Experimental Biology

The Plant Journal (2015) **84,** 1206–1218 doi: 10.1111/tpj.13073

Ribosome profiling reveals dynamic translational landscape in maize seedlings under drought stress

Lei Lei[1, 2,†], Junpeng Shi[1,†], Jian Chen[1], Mei Zhang[1], Silong Sun[1], Shaojun Xie[1], Xiaojie Li[1], Biao Zeng[1], Lizeng Peng[1], Andrew Hauck[1], Haiming Zhao[1], Weibin Song[1], Zaifeng Fan[2] and Jinsheng Lai[1,*]

[1]*State Key Laboratory of Agrobiotechnology and National Maize Improvement Center, Department of Plant Genetics and Breeding, China Agricultural University, Beijing 100193, China, and*

[2]*State Key Laboratory of Agrobiotechnology and Department of Plant Pathology, China Agricultural University, Beijing 100193, China*

Received 11 September 2015; revised 30 October 2015; accepted 9 November 2015; published online 14 November 2015.
*For correspondence (e-mail jlai@cau.edu.cn).
†These authors contributed equally to this work.

SUMMARY

Plants can respond to environmental changes with various mechanisms occurred at transcriptional and translational levels. Thus far, there have been relatively extensive understandings of stress responses of plants on transcriptional level, while little information is known about that on translational level. To uncover the landscape of translation in plants in response to drought stress, we performed the recently developed ribosome profiling assay with maize seedlings growing under normal and drought conditions. Comparative analysis of the ribosome profiling data and the RNA-seq data showed that the fold changes of gene expression at transcriptional level were moderately correlated with that of translational level globally (R^2 = 0.69). However, less than half of the responsive genes were shared by transcription and translation under drought condition, suggesting that drought stress can introduce transcriptional and translational responses independently. We found that the translational efficiencies of 931 genes were changed significantly in response to drought stress. Further analysis revealed that the translational efficiencies of genes were highly influenced by their sequence features including GC content, length of coding sequences and normalized minimal free energy. In addition, we detected potential translation of 3063 upstream open reading frames (uORFs) on 2558 genes and these uORFs may affect the translational efficiency of downstream main open reading frames (ORFs). Our study indicates that plant can respond to drought stress with highly dynamic translational mechanism, that acting synergistically with that of transcription.

Keywords: maize, ribosome profiling, RNA-seq, drought stress, translational efficiency, uORFs.

INTRODUCTION

Water deficiency is one of the major abiotic stresses for crops (Ciais *et al.*, 2005; Cattivelli *et al.*, 2008). To elucidate the drought response is therefore very important for global agricultural development. Over the years, due to the relative easiness on the measurement of the products of transcription using methods like microarray (Seki *et al.*, 2002) and the high-throughput second generation sequencing based RNA-seq technology, large amounts of transcription related studies have been performed (Wang *et al.*, 2009; Kakumanu *et al.*, 2012). As a result, a series of drought responsive genes and their corresponding transcriptional responsive networks were identified in plants (Seki *et al.*, 2002; Shinozaki and Yamaguchi-Shinozaki, 2007; Harb *et al.*, 2010; Kakumanu *et al.*, 2012).

Researches in drought stress response at translational level, however, have relatively lagged behind owing to the lack of efficient tools. It was observed that polysomes, which were the indicators of active translation, shifted to monosomes in maize and tobacco under drought treatment, suggesting the potential inhibition of mRNA translation (Hsiao, 1970; Kawaguchi *et al.*, 2003). RNA blot analysis revealed that a water deficit would alter the proportion of polysomes of putative lipid transfer protein (*ltp*), Osmotin (*osm*), ribulose bisphosphate carboxylase/oxygenase small subunit (*rbcS*) and eukaryotic initiation factor 4A (*eIF4A*) compared with control in tobacco (Kawaguchi *et al.*, 2003). Based on microarray data, the translational state of ~71% of 2136 genes in Arabidopsis (*Arabidopsis*

thaliana) which were estimated by ribosome loading rate were found to have decreased under drought stress (Kawaguchi *et al.*, 2004). Due to the limitation of methodology, the overall understanding of translational response in plants has been highly limited.

A novel method called ribosome profiling had recently been developed, which can provide a single-nucleotide resolution measurement of protein synthesis through deep sequencing of ribosome protected mRNA fragments (RPFs) (Ingolia *et al.*, 2009). As a major methodological advancement, ribosome profiling has been rapidly applied to the understanding of translational landscape in various species, including mouse (Ingolia *et al.*, 2011), zebrafish (Chew *et al.*, 2013), human (Michel *et al.*, 2012), fruit fly (Dunn *et al.*, 2013), and yeast (Ingolia *et al.*, 2009; Gerashchenko *et al.*, 2012). In plants, this method was also recently applied to analyze the photomorphogenesis and hypoxia translational response in Arabidopsis (Liu *et al.*, 2013; Juntawong *et al.*, 2014). In addition, a simplified microarray based ribosome profiling was also developed to elucidate the translation processing of chloroplast genes in four nuclear mutants in maize (Zoschke *et al.*, 2013). Ribosome profiling revealed diverse mechanisms in translation by which plants achieve fine-tune regulation of gene expression under the stimulation of light (Liu *et al.*, 2013), heat (Shalgi *et al.*, 2013), hydrogen peroxide and hypoxia (Gerashchenko *et al.*, 2012; Juntawong *et al.*, 2014). These translational responsive mechanisms act through mediating ribosome density to enhance or repress translation, or even sometimes causing frameshift or stop codon readthrough (Gerashchenko *et al.*, 2012; Liu *et al.*, 2013; Shalgi *et al.*, 2013; Juntawong *et al.*, 2014). In addition, it was shown that upstream open reading frame (uORF) can be an important regulatory element in translational response (Liu *et al.*, 2013; Juntawong *et al.*, 2014).

Here, we report the generation of RNA-seq and ribosome profiling data on 14-day maize seedling before and after drought stress treatment. Our analysis showed that the progressive drought stress induced moderate correlation between the levels of gene expressional changes on transcriptional and translational levels, with less than half of the differentially expressed genes were shared by transcription and translation, and a large number of genes had significantly altered translational efficiencies under drought stress. The translational efficiency of different genes varied three orders of magnitude and was highly influenced by their sequence features. In addition, large numbers of short uORFs were identified and were shown to be potentially translated. These uORFs might repress the translation of downstream main ORFs. Our study clearly demonstrates that plants can respond to drought stress with highly dynamic translational change, which functions independently and synergistically with the transcriptional response.

RESULTS

Data generation and ribosome profiling data characteristics

To systematically examine the transcriptional and translational response to drought stress, we performed RNA-seq and ribosome profiling on both well-watered (WW) and drought-stressed (DS) maize seedlings (Figures 1 and S1a). Both data types had two biological replicates.

In total, around 240 million and 150 million ribosome profiling reads were generated for the WW and DS seedlings, respectively (Table S1). In addition, 32 and 48 million RNA-seq reads were generated for the WW and DS seedlings, respectively (Table S2). The raw reads of the ribosome profiling were firstly processed to filter out rRNA sequences as described in Experimental procedures and then aligned to the maize B73 reference genome (RefGen_v2) with Tophat (see Experimental procedures) (Schnable *et al.*, 2009; Trapnell *et al.*, 2009). Due to the large amount of rRNAs, the mapping efficiency in our study was relatively low (~12%), which was comparable with that in *Saccharomyces cerevisiae* (16%) (Ingolia *et al.*, 2009). There are high correlations between the two biological replicates ($R^2 > 0.9$) for both RNA-seq and ribosome profiling data (Figure S1b, c).

Ribosome profiling among different organisms shared several common features that are associated with the

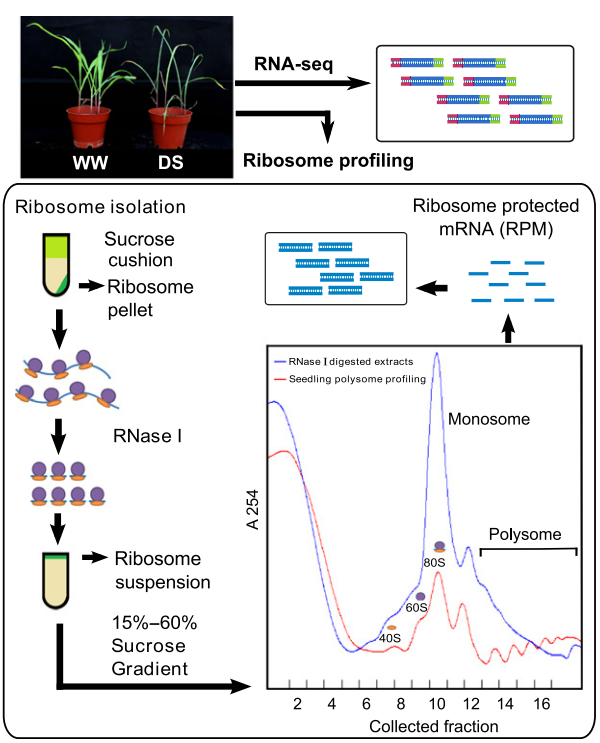

Figure 1. Overview of experimental design. RNA-seq and ribosome profiling were performed on well-watered seedlings (WW) and drought-stressed seedlings (DS).

translation mechanism and can therefore serve as hallmarks of the successful generation of ribosome profiling libraries (Ingolia *et al.*, 2009, 2011; Liu *et al.*, 2013; Juntawong *et al.*, 2014). To explore whether drought stress may affect the characteristics of ribosome profiling data, we compared them between WW and DS seedlings. We found that the length of RPF is around 30 nt in both WW and DS samples (Figures 2a and S2a), which is similar to that in mammals (Ingolia *et al.*, 2011), zebrafish (Chew *et al.*, 2013), and Arabidopsis (Liu *et al.*, 2013; Juntawong *et al.*, 2014), but slightly larger than 28 nt reported in yeast (Ingolia *et al.*, 2009). The triplet periodicity is a unique feature of read density distribution by ribosome that advances three nucleotides at a time during translation (Ingolia *et al.*, 2009; Guo *et al.*, 2010; Chew *et al.*, 2013). We observed a strong three-nucleotide periodicity when scanned after the start codon and before stop codon using the 5′-end of each read as a coordinate in both WW and DS seedlings (Figures 2b and S2b). The three-nucleotide periodicity was also clearly observed when we scanned around the start and stop codons using reads with different length separately (Figure S3a, b). Subsequently, meta-gene analysis was performed and revealed abrupt peaks of read density surrounding the start and stop codons respectively (Figure 2c). The observed peaks of RPFs indicated that the translation initiation and termination might be the rate-limiting steps for translation in maize seedlings. We also observed an excess of normalized read density right behind the peak at the beginning of CDS which can be extended to ~200 nt. It was reported that a relatively high frequency of rare codons distributed at the beginning of CDS would slow down the initial translation speed to guarantee the following sequence to be translated more smoothly with less energy consumption (Tuller *et al.*, 2010). We calculated the relative codon usage in first 150 codons and found that first five codons have lower relative codon usage (Figure S3c), which indicated a relatively higher frequency of rare codon (Wang and Roossinck, 2006). The rare codons existing at the beginning of CDS could potentially contribute the relative higher read density in this region (Figure 2c). The overall distributions of read density at the beginning of CDS (the first 200 nt) between WW and DS seedlings were highly similar (Figure 2c), different from that observed in yeast under hydrogen peroxide stress or in mammalian cell with heat treatment, in which stress induced more ribosome accumulation at the

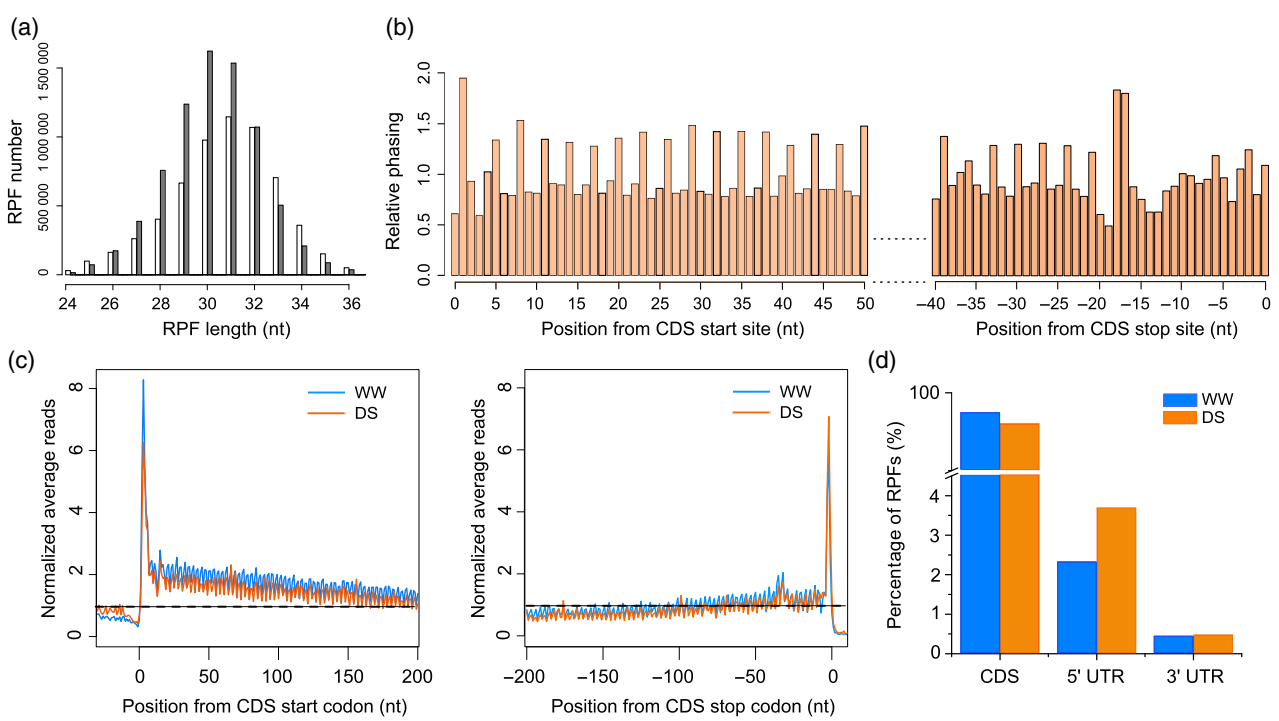

Figure 2. The characteristics of ribosome profiling data in DS seedlings.
(a) Length distribution of ribosome protected fragments (RPFs) in DS seedlings. The grey and white bars refer to two biological replicates.
(b) Three-nucleotide periodicity at the first 50 nt and the last 40 nt of CDS in DS seedlings.
(c) Meta-gene analysis of RPF density along CDS start (left) and stop codon regions (right) in WW (blue) and DS (orange) seedlings, respectively. The dash lines indicated normalized average read density which equals 1.
(d) The percentage of RPF reads located in CDS, 5′UTR and 3′UTR in WW (blue) and DS (orange) seedlings, respectively.

beginning of translation (Gerashchenko *et al.*, 2012; Shalgi *et al.*, 2013).

Until now, many small ORFs in the untranslated regions (UTRs) were identified among several eukaryotes, such as yeast (Young *et al.*, 2015), mammalian and plants (Hayden and Jorgensen, 2007; Barbosa *et al.*, 2013). Here, 2.1% and 0.4% of RPFs were observed in the 5′UTR and 3′UTR respectively while 97.5% of RPFs located in CDSs in the WW seedlings (Figure 2d). The proportion of reads mapped to CDS decreased to 95.9% while the proportion in 5′UTR and 3′UTR increased to 3.6% and 0.5% respectively under drought condition (Figure 2d). The fact that RPFs mapped to UTRs, especially in 5′UTR, indicated the potential translation in UTR, which is consistent with the reports in yeast and Arabidopsis (Ingolia *et al.*, 2009; Liu *et al.*, 2013).

Drought stress altered expression at both transcriptional and translational levels

It is well known that drought stress physiologically represses plant growth by having less biomass accumulation per unit area and lower rates of photosynthesis (Degenkolbe *et al.*, 2009; Harb *et al.*, 2010; Kakumanu *et al.*, 2012). With both RNA-seq and ribosome profiling data of seedlings that were grown under WW and DS conditions, we were able to examine the effects of drought stress on gene expression at both transcriptional and translational levels simultaneously.

Firstly, we investigated drought stress induced gene expression changes at the transcriptional and translational levels separately. We detected 1646 up-regulated genes and 2870 down-regulated genes at transcriptional level. Meanwhile, 1779 up-regulated genes and 3832 down-regulated genes were detected at translational level (Figure 3a). The number of down-regulated genes was greater than the number of up-regulated genes at both transcriptional and translational levels, which indicates a general reduction of gene expression at both levels. To confirm the translational repression, polysome profiling was performed as shown in Figure 3(b). Compared with the WW seedlings, the proportion of polysome in the DS seedlings decreased from 49.9% to 33.9% and the monosome proportion increased from 34.9% to 48% correspondingly, clearly demonstrating a genome-wide repression of translation in DS seedling (Figure 3b).

Next, we performed functional analysis of differentially expressed genes based on the MapMan software. It observed that the enriched pathways at the transcriptional and translational levels were largely overlapped (Figure S4). For example, genes enriched in pathways such as photosynthesis (Hayano-Kanashiro *et al.*, 2009), lipid metabolism, major carbohydrate (CHO) metabolism, cell wall (Kakumanu *et al.*, 2012), DNA synthesis and signaling were prominently down-regulated (Figure S4). Meanwhile, sucrose degradation, glutamate family synthesis, and stress relevant pathways were up-regulated (Figure S4) (Seki *et al.*, 2002; Kakumanu *et al.*, 2012).

It is worthwhile to note that large numbers of genes of enriched pathways showed a discordant response at transcriptional and translational levels (Figure S4). Figure 3(c) indicated that less than half of responsive genes (26.2% of up-regulated and 39.3% of down-regulated genes) were shared between transcriptional and translational levels (Figure 3c), which supported that discordant change at the two levels took place. For example, *Lhcb3* (chlorophyll *a*/*b* binding protein 3, GRMZM2G155216) was clearly observed to be repressed at only translational level (Figure S5a). 60S ribosomal protein L38 (AC190609.3_FG002) was detected

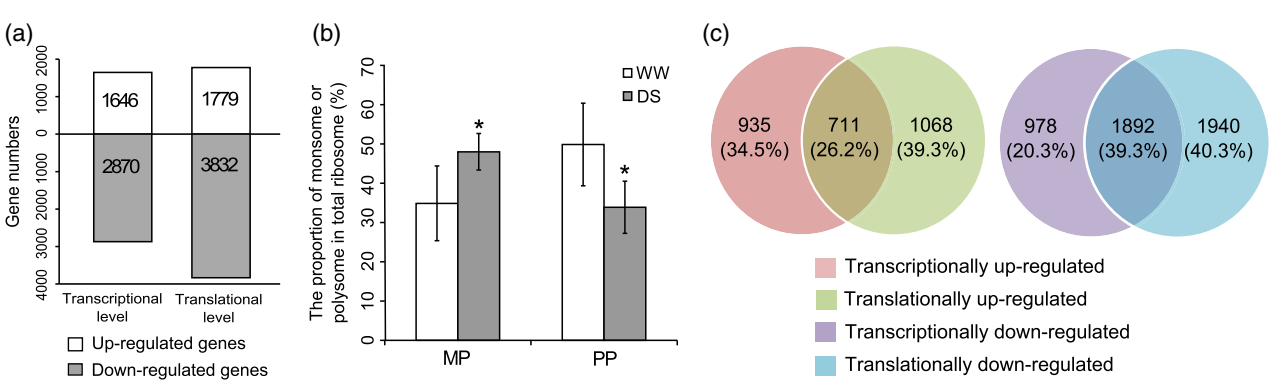

Figure 3. Drought stress induced transcriptional and translational responses.
(a) The number of differentially expressed genes (fold change ≥2 and *q*-value ≤0.01) at transcriptional or translational levels under drought stress. The white and grey bars refer to the number of up-regulated and down-regulated genes respectively.
(b) Drought stress decreased the proportion of polysomes. MP stands for the proportion of monosome and PP indicates the proportion of polysome. The white and grey bars indicate MP (or PP) in WW and DS seedlings respectively. The mean values and standard deviation were from four independent experiments. Student's *t*-test was used for hypothesis testing. Single asterisk indicates a *P*-value <0.05.
(c) The relationship between drought responsive genes at transcriptional and translational levels. Genes analyzed in Figure 3(c) were derived from Figure 3(a).

to be up-regulated at the translational level without obvious change at the transcriptional level (Figure S5b). To access the overall trend of expression changes at two different levels simultaneously, we calculated the fold change of gene expression (FPKM) at both transcriptional and translational levels. Our results showed that the changes at transcriptional and translational levels were moderately correlated (R^2 = 0.69; Figure 4). We then classified genes based on the fold change of FPKM ($|\log_2(\text{fold change})| > 1$ as cutoff) into nine gene categories (Figure 4). Further analysis revealed that 59% of the responsive genes were among the accordant groups (classes C and G) which were co-regulated with their expression increased or decreased to a similar extent at both transcriptional and translational levels. Meanwhile, 41% of responsive genes (1832 genes) were located in the other six discordantly regulated groups (classes A, B, D, F, H, and I; Figure 4).

Genes in four discordant regulated groups were further analyzed for Gene Ontology (GO) enrichment. Genes in classes D and F were regulated at transcriptional level without significant change in translation. Among them, 319 transcriptionally down-regulated genes in class D were enriched in metabolic and cellular processes (carboxylic acid biosynthesis and glycolysis) (Figure S6a and Table S3), while 399 transcriptionally up-regulated genes in class F were observed to be enriched in heat shock protein binding (Figure S6b and Table S3). In contrast, genes in classes B and H were regulated translationally without detectable change at mRNA levels. In class H, 589 genes with decreased translation were remarkably enriched for membrane, transferase activity, and modification (Figure S6c and Table S3). There were 525 translationally up-regulated genes (class B), involved in the pathways of gene expression, ribosome, RNA binding, and translation (Figure S6d and Table S3).

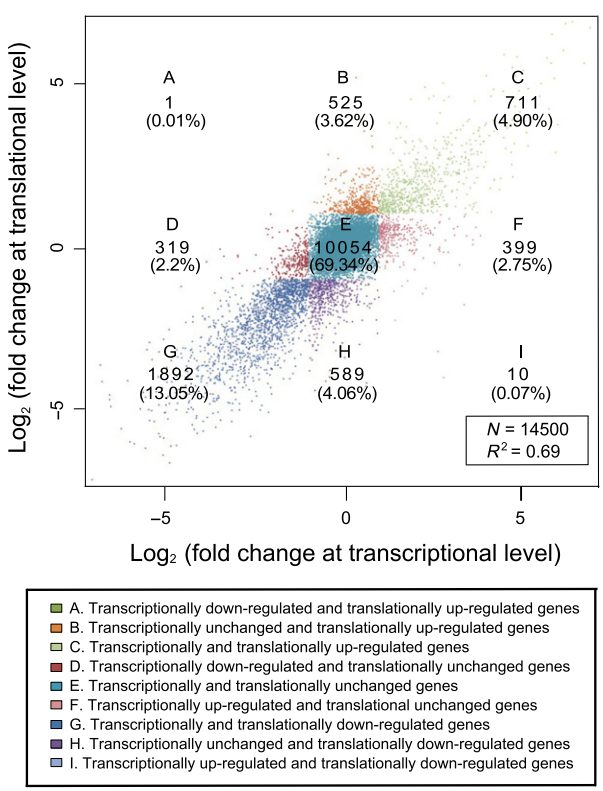

Figure 4. Fold changes of FPKMs at transcriptional and translational levels under drought stress.
Nine squares in different colours indicated nine responsive groups (fold change ≥2 and *q*-value ≤0.01).

Drought stress introduced significant changes of the translational efficiencies of a large number of genes

Translational efficiency (TE, calculated by $\text{FPKM}_{\text{ribosome-profiling}}/\text{FPKM}_{\text{RNA-seq}}$), which directly measures the efficiency of RNA utilization, is an important index for translation (Ingolia *et al.*, 2009; Dunn *et al.*, 2013). 100 bp pair-end (PE) RNA-seq data was used to measure the transcriptional abundance in maize for its higher mapping accuracy compared with single-end reads. To answer whether any bias may be generated as we have used different read length (100 bp versus 26–34 bp) and sequencing strategy (pair-end versus single-end) between RNA-seq and ribosome profiling data, we simulated 30-bp single-end (SE) RNA-seq reads from the 5′-end of 100 bp PE data for the WW seedling. Then, we compared it with our 100 bp PE RNA-seq data (see Experimental procedures). We found that the transcriptional abundance (FPKMs) and TE calculated from 100 bp PE and 30 bp SE RNA-seq data were highly correlated (Figure S7a, c). Also, the distributions of FPKM of all expressed genes were almost identical (Figure S7b). However, due to different methods of fragmentation and recovery used for cellular and ribosome protected mRNA, there may be potential bias for some particular mRNA fragments.

Genome-wide TE analysis showed that TE of genes varied more than ~4000-fold, which suggested that a large number of genes underwent a highly dynamic translational regulation (Figure 5a). For example, photosynthesis genes were among the most active pathways in rapidly growing seedlings and reported to have a relative high transcriptional abundance (Li *et al.*, 2010). We observed both higher transcriptional abundance (*P*-value = 6.45e-13) and higher TE (*P*-value = 2.64e-08) for genes known to be involved in photosynthesis as compared to the all other genes expressed in seedlings (Figure 5a). The increased TE of these photosynthesis related genes indicated a further increase of translation efficiency on top of their high activity of transcription during rapid growth of seedling.

We next tried to explore whether plants can response to drought stress through the change of translational efficiency. Although, the global distribution of mRNA abun-

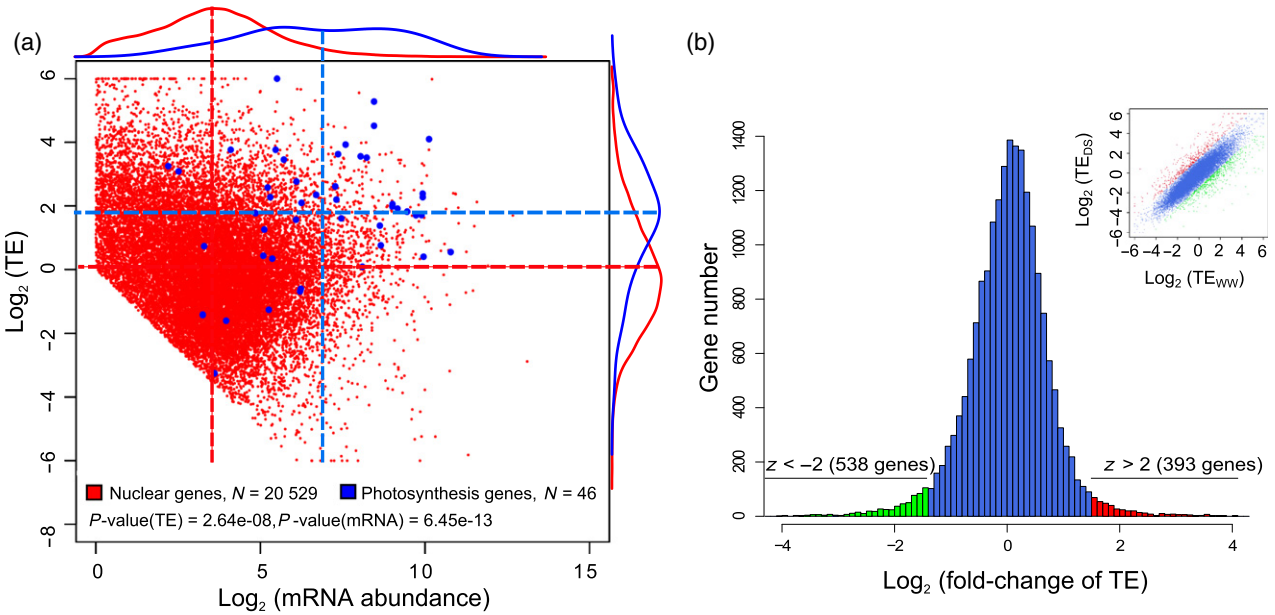

Figure 5. Genome-wide translational efficiency (TE) analysis.
(a) An overview of the $\log_2$(TE) as a function of mRNA abundance in WW seedlings. The density is shown along the axes. Red and blue colours represent nuclear genes and photosynthesis genes respectively. The red and blue dash lines indicate mean value of corresponding genes. *P*-values were determined by single-tailed Student's *t*-test.
(b) Histogram of the fold change in TE between WW and DS seedlings. The inset figure shows an overview of the TEs in WW and DS seedling. Red and green colours indicate genes with significantly increased and decreased TE respectively. A *z*-score greater than 2 was adopted as the threshold for both the main figure and the inset figure.

dance and TE were highly similar between the DS seedlings and the WW seedlings (Figure S8a), we still detected 538 genes with decreased TE (less than 2.8-fold, *z*-score < -2) and 393 genes with increased TE (more than 2.7-fold, *z*-score > 2) after drought treatment (Figure 5b), demonstrating that adjusting gene translational efficiency can be an important way of stress responses for plants.

As the transcriptional and translational abundance both contributed to the translational efficiency, we next checked the distribution of gene with decreased and increased TE in previous determined nine responsive categories to dissect the change of TE at transcriptional and translational levels respectively. As expected, the changes of transcriptional and translational abundance could both contribute to the changes of TE as showed in Figure S8(b, c). While, genes which were solely regulated at transcriptional or translational levels accounted for more than half of the genes which TE significantly changed. For example, genes in groups F (solely regulated at transcriptional level) and H (solely regulated at translational level) together comprised about 65% of the genes with significantly decreased TE (*z*-score < -2) (Figure S8b). In addition, a proportion of genes accordantly regulated at transcriptional and translational levels (groups C, E and G) can also lead to a significant change of TE, due to a different degrees of fold changes between transcriptional and translational abundance (Figure S8b, c).

The translational efficiencies of genes were affected by their sequence features

Sequence features of genes were reported to contribute to the proportion of mRNAs associated with polysomes and further affect protein abundance (Ringner and Krogh, 2005; Vogel *et al.*, 2010; Liu *et al.*, 2012). To understand the specific contribution of sequence features in translational regulation in maize, we examined three sequence characteristics (sequence length, normalized minimal free energy (NMFE) and GC content) in CDS, 3′UTR, and 5′UTR of genes, and estimated their potential effect on translational efficiency of corresponding genes (see Table S4). For CDS, we observed that genes with higher translational efficiency (Log_2(TE) > 1) tend to have shorter length, higher GC content, and lower NMFE (Figure 6a). For 3′UTR, the differences were relatively minor between higher and lower translational efficiency genes. Only genes in highest translational efficiency group (Log_2(TE) > 1) tend to have shorter length (Figure S9b), higher GC content and lower NMFE in 3′UTR than other groups (Figure S9a, c). For 5′UTR, however, genes with higher translational efficiency (Log_2(TE) > 1) were found to hold the 5′UTR with a higher NMFE, shorter length and lower GC content (Figure S9d–f). The sequence features of genes in different TE groups in DS seedlings were consistent with the trends in WW seedlings (Figure S9 g–i).

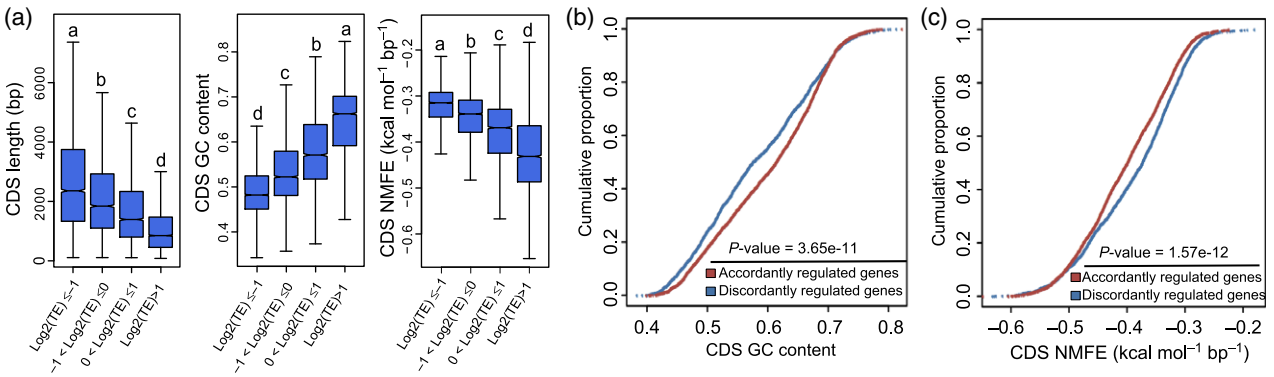

Figure 6. The influence of sequence feature on translational efficiency.
(a) The difference of coding sequence (CDS) length, GC content and NMFE (normalized minimal free energy) among four TE groups. The letters a–d indicate significant differences based on Student's *t*-test (*P*-value <0.05).
(b, c) Graphs show the difference in CDS GC content (b), and NMFE (c) between accordantly (red) and discordantly (blue) regulated genes at transcriptional and translational levels. *P*-values were determined by the Kolmogorov–Smirnov test.

Next, we checked whether genes with accordantly and discordantly expressed patterns differed in their sequence features. Based on the Kolmogorov–Smirnov test (KS test), the cumulative curve illustrated that genes located in accordant group (genes in the overlapped parts in Figure 3c) tended to have a higher GC content (*P*-value = 3.7e-11) and lower NMFE (*P*-value = 1.6e-12) in CDSs when compared with discordant ones (genes in the non-overlapped parts in Figure 3c) (Figure 6b, c). Also, genes with a lower GC content in 5′UTRs tended to be accordantly regulated (*P*-value = 1.2e-4; Figure S9j).

Widespread upstream open reading frames (uORFs)

Water deficiency increased the proportion of RPFs in 5′UTRs by 1.7-fold (Figure 2d), similar to what was observed in yeast under starvation or oxidative stress (Ingolia *et al.*, 2009; Gerashchenko *et al.*, 2012), and in mouse fibroblast under heat shock stress (Shalgi *et al.*, 2013). These observations implied that some elements located in 5′UTR could participate in the stress response. uORFs, which consist of small open reading frames in 5′UTRs, are well known to repress the translation of the downstream main ORFs (mORFs) by reinitiation and leaky scanning and have been identified in several organisms (Morris and Geballe, 2000; Sachs and Geballe, 2006; Barbosa *et al.*, 2013; von Arnim *et al.*, 2014). However, only uORFs of two classical genes (*Lc* and *O2*) have been identified previously in maize (Ludwig *et al.*, 1989; Damiani and Wessler, 1993; Lohmer *et al.*, 1993; Wang and Wessler, 2001). The ribosome profiling data generated in this study made it possible to identify uORFs on a genome-wide scale in maize.

We firstly performed uORF prediction across the maize genome based on the presence of AUG start codons in 5′UTR sequences. To identify uORF-containing genes accurately, we focused on 26 971 maize genes in filtered gene set (FGS) that are syntenic with four other grass species: rice (*Oryza sativa*), brachypodium (*Brachypodium distachyon*), foxtail millet (*Setaria italica*), and sorghum (*Sorghum bicolor*). As a result, 7927 (~30% of syntenic genes) were predicted to have uORFs, with an average of 2.8 uORFs per gene and a median length of 36 bp (Figure S10a, b). Among them, 2558 genes (including 45 classical genes like *Lc*) were shown to have 3063 ribosome-binding uORFs with median length of 105 bp (potentially translated uORFs) in seedlings under normal growth conditions (Table S5 and Figure S10c, d).

Translated uORF repressed the translation of mORFs

To depict the characteristic differences between translated and untranslated uORFs, three parameters related to the reinitiation of the mORF were compared: uORF length, length of 5′UTR, and NMFE (Sachs and Geballe, 2006; Barbosa *et al.*, 2013). We found that the translated uORFs had a longer length (*P*-value < 2.2e-16) and stronger folding potential (*P*-value < 2.2e-16) than untranslated ones (Figure 7a, c). However, genes with translated uORFs displayed a shorter 5′UTR length (*P*-value < 2.2e-16; Figure 7b). Further refining the influence of 5′UTR length, we observed that both the relative distance from the uORF to the start codon of the mORFs (*P*-value < 2.2e-16), and from the uORF to the transcription start site (TSS) (transcription start site; *P* = 1.4e-9) in translated uORFs were shorter (Figure 7d, e). The differences of sequence characteristics between translated and untranslated uORFs in DS seedlings were consistent with that in WW seedlings (Figure S11a–e).

Kozak consensus sequence with 'GCCA/GCCAUGG,' especially the position of −3(A/G) and 4(G) around AUG start codon is important for start codon recognition as well as translation initiation (Kozak, 1986, 2002). We firstly performed motif analysis around the start codon of all FGS

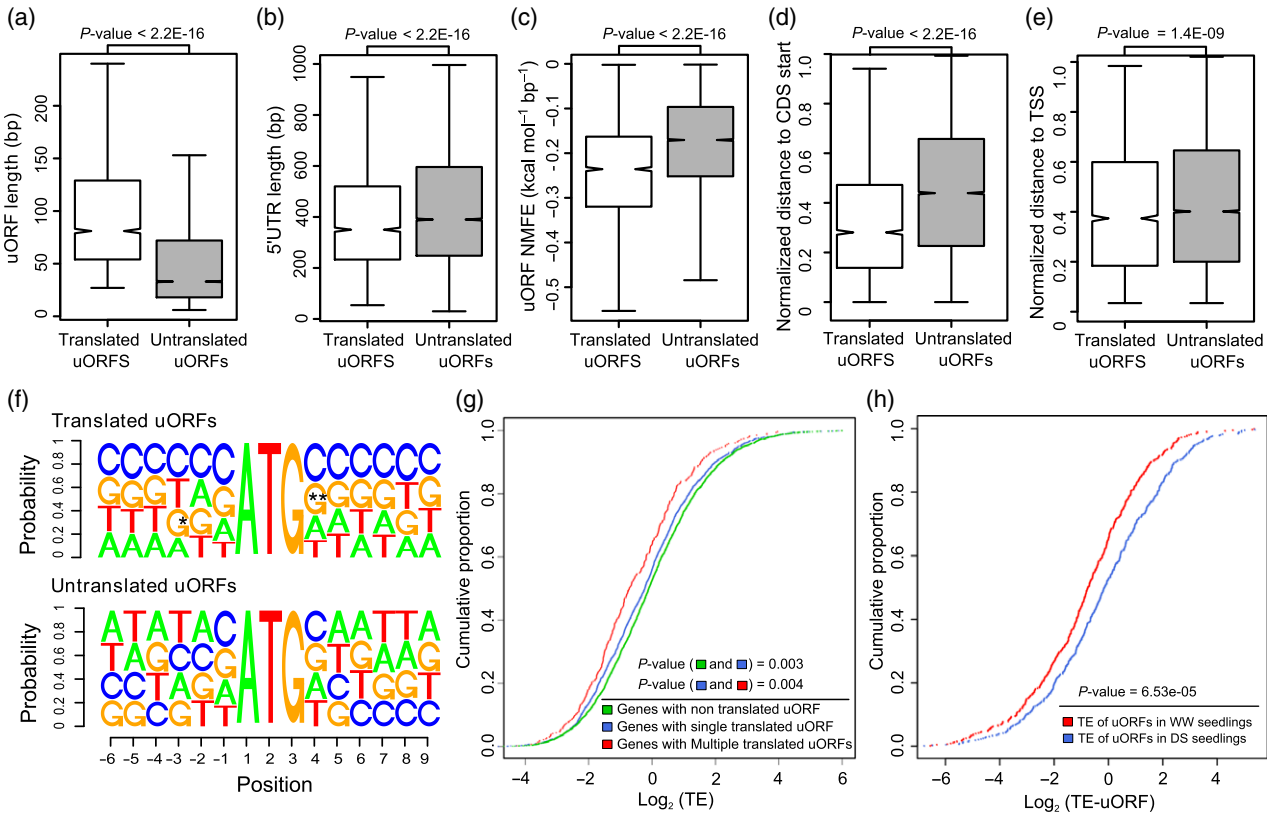

Figure 7. Characteristics of uORFs in WW seedlings.
(a–e) In the figure parts (a) to (e) show the difference between translated and untranslated upstream open reading frames (uORFs) in uORF length (a), 5′UTR length (b), NMFE (c), normalized distance from uORFs to CDS ATG start codon (d), and normalized distance from uORFs to the transcription start site (TSS) (e). White and grey colours indicate translated and untranslated uORFs respectively. *P*-values were determined by Student's *t*-test.
(f) Sequence composition between translated (top) and untranslated uORFs (lower) around the ATG start codon. Chi-squared test was used for significance analysis. Single and double asterisks indicate *P*-value <0.05 and *P*-value <0.01 respectively.
(g) The difference of TE among genes with none (green), one (blue) and multiple translated uORFs (red).
(h) The difference of uORFs' TE between WW (red) and DS (blue) seedlings. *P*-values in (g) and (h) were determined by Kolmogorov–Smirnov tests.

transcripts. The flanking sequence of start codon in FGS genes coincided well with Kozak sequence (Figure S11f). Subsequently, we compare the frequency of each base of the flanking sequence around uORF start codon between translated and untranslated ones. A high GC content of the flanking sequence in translated uORFs was observed (Figures 7f and S11 g). Furthermore, the probabilities of guanine at the position of −3 (*P*-value = 0.02) and +4 (*P*-value = 3.0e-4) in translated uORFs were found to be higher than in untranslated ones (Figure 7f).

In order to investigate the influence of the translated uORFs upon the translation of the mORFs in maize, we next analyzed the TE of three groups of genes: genes with predicted uORFs but without translation, genes with one, and with multiple translated uORFs. Compared with untranslated uORFs, translated uORFs significantly decreased the TE of corresponding genes (Figure 7g). Also, the reduction of TE was shown to be further enhanced by the increasing of the number of translated uORFs (Figure 7g).

uORFs were reported to response to sugar signal (Wiese *et al.*, 2004), light (Liu *et al.*, 2013) and pathogen infection (Pajerowska-Mukhtar *et al.*, 2012). Then, we analyzed the translational efficiency of uORFs in DS seedling. Compared with WW seedling, the TE of uORFs was higher in DS seedlings which indicated the translation of uORFs was enhanced globally under drought stress in maize (Figure 7h). The increased TE of uORF was consistent with the increased proportion of RPFs located in 5′UTR (Figure 2d).

DISCUSSION

Transcriptional and translational responses working together on drought stress

By having successfully obtained the ribosome profiling and RNA-seq data, we are not only able to address the genome-wide gene expression changes at the translational level after drought stress but also to investigate the interplay between transcriptional and translational responses. In general, we observed a relative high Pearson correlation

between the fold changes of gene expression of the transcription and translation under progressive drought condition (Figure 4).

However, we observed 1832 genes (41% of drought responsive genes) underwent discordant change at the transcriptional or translational levels, which clearly indicated independent stress responses at the two levels (Figure 4). There were 1114 genes that were exclusively regulated at translational level. Translational response do not need to produce new mRNA, therefore it can be a more rapid and direct way of environmental response (Sonenberg and Hinnebusch, 2009). So despite being a fine-tuning role as discussed before (Lackner *et al.*, 2012), translation itself apparently plays a relatively independent role in stress response. On the other hand, we identified 718 genes in classes D and F that are exclusively regulated on transcriptional level without detectable change of translation. These genes are primary function in basic physiological processes. As reported in yeast with sodium chloride treatment, the mRNA abundance at a denote time point was better correlated with the abundance of protein at its following time point than with that of the same time point, demonstrating that the protein expression had lagged behind the transcription in stress response (Lee *et al.*, 2011). Therefore, we hypothesize that the change of the mRNA abundance of a group of genes in classes D and F can be an indicator for the follow-up change of translation. For the 399 genes observed with only increasing in transcription in class F, it also could be that plants can modulate mRNA abundance to make up the reduction of translational efficiency to maintain the essential processes running. Another potential explanation is that the increased mRNA abundance could form a reserved pool for quick translation in the future once the stress relieves (Shenton *et al.*, 2006). Above all, the interweaving between the transcriptional and translational response increases the flexibility of gene expression, which is of benefit to adaptation. It is possible that rapid and severe stress may lead to quick and independent gene expression responses at both transcriptional and translational levels; while chronic, moderate stress may result in more coordinated regulation at both levels.

Sequence features of genes can have effects on the translational efficiency

Except for the function of encoding proteins, genomic sequences contain large amounts of information for expression regulation. In this study, we found that genes with different translational efficiency were observed to have different sequence features, especially the features in the CDS in both WW and DS seedlings (Figures 6a and S9 g). These sequence features also were found to be associated with different gene expression patterns under drought stress (Figures 6b, c and S9j).

Previous research revealed that UTRs of genes contain a number of translational regulatory elements. uORF in 5′UTR is a *cis*-element which were widely reported to have function on translation repression (Lohmer *et al.*, 1993; Wang and Wessler, 1998; Wiese *et al.*, 2004). We here observed that maize uORFs decreased the translational efficiency of the mORFs on a genome-wide scale (Figure 7g). Internal ribosome entry site (IRES) which initiate gene translation by cap-independent mechanism under stress is another type of regulatory element in 5′UTR (Spriggs *et al.*, 2008). It was reported that the IRES of alcohol dehydrogenase-1 (*Adh1*) in maize was also active in tobacco plants and *in vitro* translation systems (Mardanova *et al.*, 2008). Besides, the translation of several genes in Arabidopsis sharing two motifs (TAGGGTTT and AAAACCCT) in the 5′UTR was found to be enhanced after light and hypoxia treatment (Liu *et al.*, 2013). Experimental evidence further proved that the two motifs could respond to both light and hypoxia by increasing downstream gene expression *in vitro* (Liu *et al.*, 2013). It is possible that many of these *cis*-elements in UTR would be identified in maize in the future. In addition, codon usage, poly(A) tail length and potential secondary structure were reported to be involved in translational response (de Sousa Abreu *et al.*, 2009; Spriggs *et al.*, 2010; Tuller *et al.*, 2010). Much of these regulatory mechanisms are still waiting to be identified in plants.

Diverse mechanisms of uORF-mediated translation repression

In this study, we found that uORFs repressed the translation of the mORFs and the repression was enhanced by increasing the number of translated uORFs (Figure 7g). This phenomenon was also observed in Arabidopsis (Liu *et al.*, 2013). Besides, multiple uORFs in mammalian were reported to inhibit protein accumulation more seriously than transcripts with one or none uORF based on mass spectrometry data (Calvo *et al.*, 2009).

uORFs in plant and mammalian may share a similar translation repression mechanism which could be divided into two categories: competing with the downstream mORFs for translational initiation complex and affecting mORF's reinitiation. The start codon of uORFs can strongly compete with that of mORF's for translation initiation complex and whether the start codon of uORF could be efficiently recognized is the key for uORF-mediated repression (Sachs and Geballe, 2006; Barbosa *et al.*, 2013). Our results suggested that the sequence flanking ATG was perfectly accorded with Kozak sequence in mORFs (Figure S11f). The sequence flanking ATG of translated uORFs was found to be less conserved with Kozak sequence while that for the untranslated uORFs were least conserved (Figure 7f). Therefore, the start codons of uORFs have the possibilities of being either ignored or recognized.

Once being ignored, it would lead to leaky scanning and the translation of mORFs. However, if they were recognized, the translation elongation and termination of uORFs would turn out to be the barriers for the reinitiation of mORFs (Calvo *et al.*, 2009; Barbosa *et al.*, 2013). uORFs with longer length and shorter distance from uORF to the mORF were thought to be unfavourable for the reorganization of eIF-GTP-Met-tRNA ternary complex, which was essential for the translation initiation of the mORFs, so that the inhibition could be more efficient (Sachs and Geballe, 2006). The observation of translated uORFs with longer length and a shorter distance from uORF to CDS start than untranslated ones in this study supported this view (Figure 7a, d). Besides uORF length, sequence context of uORF was also found to be associated with uORF's function in plant. A conserved uORF of *GGP* in kiwifruit and Arabidopsis could respond to high concentration of ascorbate and repress *GGP* translation in a sequence-dependent manner (Laing *et al.*, 2015). In another case, two overlapping conserved uORFs of *AdoMetDC1* in Arabidopsis could mediate ribosome arrest at translation termination and further trigger nonsense-mediated decay to respond to the change of polyamine level (Uchiyama-Kadokura *et al.*, 2014). Additionally, uORF encoded peptide was reported to act in *cis* to repress the translation of the mORFs. A heptapeptide encoded by an uORF (*gDcADC8*) in carnation could repress the translation of the mORFs in *cis* both *in vivo* and *in vitro* (Chang *et al.*, 2000). Very recently, frameshift mutants revealed that 11 CPuORFs (conserved peptide uORF) encoding peptides acted in *cis* to inhibit the translation of the mORFs in Arabidopsis (Ebina *et al.*, 2015).

Upon the analysis of high-throughput RNA-seq and ribosome profiling data, our work reveals a highly dynamic translational landscape of maize in response to drought stress. However, methods used for most of the ribosome profiling studies had measured the translational abundance inferred from the monosomes digested from the all ribosome protected mRNAs, which may risk the possibility of overestimation (Ingolia *et al.*, 2009; Gerashchenko *et al.*, 2012; Liu *et al.*, 2013). Direct measuring of the polysome protected mRNA is therefore highly recommended if it is applicable (Juntawong *et al.*, 2014).

EXPERIMENTAL PROCEDURES

Plant materials

The seeds of maize (*Zea mays*) inbred line B73 were sterilized by immersion in 10% hydrogen peroxide for 30 min followed by six washes in distilled water. The seeds were placed on the paper towel at 28°C for 24 h, and then, transplanted to pots containing a mixture of vermiculite and soil (1:1, v/v). Seedlings were grown in a greenhouse at condition of 30°C for 16 h light and 25°C for 8 h of darkness. A progressive drought stress was introduced after sowing 4 days by water deficit until day 14. Aerial tissues were harvested, immediately frozen in liquid nitrogen, and stored at −80°C. Leaf tissues of 14 day WW and DS seedling were collected for relative water content (RWC) determination to measure the extent of drought treatment (Raymond Hunt *et al.*, 1987).

Ribosome profiling

The method of ribosome isolation was adapted from Mustroph and modified by Li (Mustroph *et al.*, 2009; Li *et al.*, 2013). Tissue powder (2 g) was added to 10 ml PEB and homogenized (200 mM Tris–Cl (pH 9), 200 mM KCl, 25 mM EGTA, 35 mM $MgCl_2$, 0.2% Brj-35, 0.2% TritonX-100, 0.2% Igepal CA630, 0.2% polyoxyethylene 10 tridecyl ether, 5 mM DTT, 100 mg ml^{-1} cycloheximide, 100 mg ml^{-1} chloramphenicol, and a complete proteinase inhibitor cocktail). The homogenate was passed through double layers of miracloth followed by centrifugation at 10 000 ***g*** for 15 min at 4°C. The supernatant was transferred and filtered through two layers of miracloth. The filtrate was layered on top of a 1.7 M sucrose cushion and centrifuged at 170 000 ***g*** for 3 h at 4°C. The ribosome pellet was resuspended in RB (Mix 20 mM Tris–Cl (pH 8.0), 150 mM NaCl, 5 mM $MgCl_2$, 1 mM DTT and 100 μg ml^{-1} cycloheximide, 100 μg ml^{-1} chloramphenicol).

Ribosome profiling was adapted from Ingolia (Ingolia *et al.*, 2012). In total, 600 μL ribosome solution at the value of 2 (A_{260}) was used to digest at the condition of room temperature for 1 h with adding 15 μl RNase I (Invitrogen, cat. no. AM2294, http://www.thermofisher.com/cn/zh/home/brands/invitrogen.html), then stopped by adding 20 μl RNase inhibitor (Invitrogen, cat. no. AM2694). Monosomes were collected by sucrose density gradient centrifugation at 50 000 rpm (Beckman, SW55.1 rotor) for 1.5 h at 4°C. RNA protected fragments were extracted according to the manual introduction of miRNeasy RNA isolation kits (Qiagen cat. no. 217004, http://www.qiagen.com/). The RNA samples were then subjected to 15% (wt/vol) polyacrylamide TBE-urea gel electrophoresis and purified with the indication of oligoribonucleotide chains: 5′-AUGUACACGGAGUCGAGCUCAACCCGCAACGCGA-(Phos)-5′ and 5′-AUGUACACGGAGUCGACCCAACGCGA-(Phos)-3′ (TaKaRa). Universal miRNA linker was added to the purified RNA fragments (New England Biolabs, cat. no. S1315S, https://www.neb.com/). The ligation products were subjected to reverse transcription and circularization. Sequence libraries were ultimately obtained through PCR amplification. Ribosome profiling libraries were sequenced on an Illumina Hiseq 2500 platform to generated single-end 50 nt reads.

Polysome profiling

For polysome profiling, 1500 units OD_{260} of ribosome solution was loaded on a sucrose with the gradient of 20–60% (w/v) and performed ultracentrifugation at speed of 46 000 rpm (Beckman, SW55.1 rotor) for 1.5 h at 4°C. Gradient Profiler (BioComp, http://www.biocompinstruments.com/index.php) which contained EM-1 UV data acquisition system (Bio-Rad, http://www.bio-rad.com/) was employed for component analysis according to the manufacturer's instructions.

mRNA sequencing library construction

Total RNA was extracted using TRIzol reagent (Invitrogen). RNA-seq libraries were prepared according to the manufacturer's protocol of the Illumina Standard mRNA-seq library preparation kit (Illumina, http://www.illumina.com/). RNA-seq libraries were sequenced by paired-end 2*101 nt (both ends with 101 nucleotides long) on an Illumina HiSeq 2500 platform.

Processing and alignment of ribosome profiling raw data

Raw reads were filtered by fastq_illumina_filter (version 0.1) with parameters –keep N -v to keep better quality reads. Adapter

sequence (5′-CTGTAGGCACCATCAAT-3′) were trimmed out by fastx_clipper with parameters –Q 33 -a CTGTAGGCACCATCAAT -l 25 -n -v, then fastx_trimmer with parameters –Q 33 -f 2 was used to trim out the first nucleotide from 5′-end of each read for the reason that it frequently represents an untemplated addition during reverse transcription. We downloaded the rRNA reference sequence from NCBI by searching the keywords 'ribosomal DNA', then aligned reads against rRNA reference sequence by bowtie (version 0.12.9) with parameters –chunkmbs 1000 -un -al to filter out reads derived from rRNAs (Langmead *et al.*, 2009). Cleaned reads were mapped to maize B73 genome (RefGen_v2) by Tophat (v2.1.0) with parameters –bowtie1 -N 2 -l 50000 -p 3. Mapping efficiency was defined as the number of mapped reads divided by the number of total input reads (Trapnell *et al.*, 2009).

Calculation of translational abundance

Translation abundance of each gene was calculated by Cufflinks (v2.2.1) with parameters –p 3 -G -u (Trapnell *et al.*, 2009). Only reads located in CDSs were used to calculate translational abundance. -u option was used to more accurately weight reads that mapped to multiple locations by a 'rescue method'. FPKM was used to measure the translational abundance of each gene.

Alignment of 100 bp pair-end RNA-seq data, calculation of transcriptional abundance and the simulation of 30 bp single-end RNA-seq data for comparison with 100 bp PEs

Here 100 bp pair-end RNA-seq data were aligned to maize B73 genome (RefGen_v2) by Tophat (v2.1.0) with parameters –bowtie1 -N 2 -l 50000 -p 3. Transcriptional abundance was measure by FPKMs by Cufflinks (v2.2.1) with parameters –p 3 -G -u. Only reads located in exons were used to calculate transcriptional abundance. For the simulation of 30 bp single-end RNA-seq data, we randomly extracted the sequence from the 5′-end of each read with length ranged from 26 bp to 34 bp. The alignment and FPKM calculation were performed as above. Pairwise Pearson correlation was used to measure the association of transcriptional abundance between 100 bp PE RNA-seq and 30 bp SE RNA-seq data.

Correlation between two replicates of transcriptional and translational abundance, calculation of translational efficiency (TE)

Only genes with FPKM ≥1 at transcriptional and translational levels were used to calculate the Pairwise Pearson correlation (R^2) between two replicates. TE was calculated by $FPKM_{(translational\ level)}/FPKM_{(transcriptional\ level)}$ with the FPKMs at two levels ≥1. Log2 transformed TEs were used to show the TE distribution of genes.

3-nt periodicity, ribosome A-site calibration and meta-gene read depth analysis

The ribosome profiling reads were used to analyze the 3-nt periodicity, calibrate the A-site position and perform meta-gene read depth analysis. Due to the high reproducibility of two replicates, we merged them and got the unique mapped reads according to the tag (NH:i:1) in the bam file. For the 3-nt periodicity analysis, the 5′-end of each read was accurately assigned to a relative distance to the CDS start and end. Then we got the cumulative read depth at each relative distance. Relative phasing of each site was calculated by i = 4 × read number i/(read number (i - 2) + read number (i - 1) + read number (i + 1) + read number (i + 2)), then plot the phasing value against each site to show 3-nt periodicity. Reads uniquely mapped to CDS start and end were extracted according to different read length (27~34 nt), then the read density maps were constructed to re-calibrate A-site according to the 5′-end of each read relative to the CDS start and end. The aligned reads were assigned to an A-site position based on the different length of each read. The offset from 5′-end of the alignment is 27–29 nt, +15 nt; 30–32 nt, +16 nt and 33–34 nt, +17 nt. Then, meta-gene read depth analysis was performed according to the assigned A-site position of reads that mapped around CDS start and stop. Read density at each nucleotide was firstly normalized by the average read density on each CDS, then normalized by the number of analyzable genes (FPKM ≥ 1).

The analysis of the sequence features among four groups of different translational efficiency

For the genes with multiple transcripts, the one with longest CDS was used to define the CDS of each gene. To improve the accuracy of prediction of 5′UTR and 3′UTR, only genes that were predicted to be syntenic with sorghum, foxtail millet, rice and brachypodium from MaizeGDB were used (N = 26 971). Normalized minimal free energy (NMFE) was used to define the sequence stability of secondary structure, which was calculated by RNAfold and normalized by the sequence length. The P-value of the mean value difference of sequence features between two TE groups were determined by two-tailed Student's t-test ($\alpha = 0.05$).

Identification of potential uORFs and motif exhibition around the start codon of uORFs

5′UTR of syntenic genes as mentioned above with length ranged from 30 bp to 1000 bp were used to predict uORFs with the sequence structure of (ATG-3n-TAG|TAA|TGA). Whether it was expressed of an uORF was determined by FPKM ≥ 1 using Cufflinks with parameters above. R library (SeqLogo) was used to show the motif enrichment around the start codon between expressed and unexpressed uORFs (Bembom, 2007).

Identification of differentially expressed genes and GO analysis

Cuffdiff (v2.2.1) was used to identify the differentially expressed genes at transcriptional and translational levels, respectively. We set the parameter –FDR 0.01 to control thr False Discovery Rate lower than 0.01, -u to use 'rescue method' for multiple mapped reads. Multiple testing error was controlled using the Benjamini–Hochberg correction. Only genes with q-value less than 0.01 and with the fold change of FPKM larger than 2 were defined as differentially expressed genes. Mapman (v3.5.1) was used to display the diagrams of enriched metabolic pathways of differentially expressed genes. For the GO analysis, the IDs of differentially expressed genes were put into AgriGO (http://bioinfo.cau.edu.cn/agriGO/) using *Zea mays* V5a transcripts as the background databases (Du *et al.*, 2010). The functional protein annotation was performed by InterProScan 5.

Identification of accordantly and discordantly regulated genes

We classified genes into nine categories according to the fold change and q-value reported by Cuffdiff. Genes up-regulated or down-regulated simultaneously at transcriptional and translational levels were defined as accordantly regulated genes. Other categories, except for the category without change at two levels,

were defined as discordantly regulated genes. The fold changes at transcriptional and translational levels were used to calculate the Pairwise Pearson correlation. IGV (Version 2.3.55) was used to show the expression changes at transcriptional and translational levels simultaneously.

Identification of genes with significantly changed translational efficiency (TE)

The comparison between TE and mRNA abundance on a genome-wide scale was performed according to the report (Rooijers *et al.*, 2013). To identify genes with significantly altered translational efficiency (TE) after drought stress treatment, the TEs of genes in DS seedling were divided by the ones in WW seedling, then Log2 transformed to follow Normal Distribution. Genes with a *z*-score $\geq$ 2 were defined as TE up-regulated genes. While, genes with a *z*-score $\leq$ -2 were defined as TE down-regulated genes.

Accession code: Sequencing data generated in this study have been deposited at the NCBI short Read Archive under the accession SRP052520.

ACKNOWLEDGEMENTS

We would like to express gratitude to Dr Shengben Li for sharing the experiences on ribosome isolation and digestion. We also thank Dr Nicholas Ingolia, Dr Eivind Valen and Guoliang Chew for advices on A-site calibration and Dr Mingjun Liu for his advice on the ribosome profiling data analysis. This work was supported by the 863 Project (2012AA10A305), the 948 project (2011-G15) and the National Natural Science Foundation of China (31225020; 91435206; 31421005).

SUPPORTING INFORMATION

Additional Supporting Information may be found in the online version of this article.

Figure S1. Libraries reproducibility in well-watered (WW) and drought-stressed seedlings (DS).

Figure S2. The characteristics of ribosome profiling data in WW seedling.

Figure S3. A diagram of A site calibration based on ribosome protected fragment (RPF) length.

Figure S4. MapMan functional categories of drought responsive genes enriched at transcriptional and translational levels.

Figure S5. Gene expression patterns at transcriptional and translational levels.

Figure S6. GO annotation of discordantly regulated genes under drought condition.

Figure S7. The comparison of simulated 30 bp single end (SE) data and 100 bp pair-end RNA-seq data (PE).

Figure S8. Global distribution of translational efficiency (TE) in WW and DS seedlings.

Figure S9. The TE of genes was affected by sequence features.

Figure S10. Genome-wide prediction of upstream open reading frames (uORFs).

Figure S11. The sequence features of uORFs.

Table S1. Alignment statistics for ribosome profiling reads.

Table S2. Alignment statistics for RNA-seq reads.

Table S3. List of genes in four main discordantly responsive groups.

Table S4. Numbers of genes analyzed in 4 different TE (translational efficiency) groups.

Table S5. List of genes with translated uORFs in well-watered seedlings.

REFERENCES

von Arnim, A.G., Jia, Q. and Vaughn, J.N. (2014) Regulation of plant translation by upstream open reading frames. *Plant Sci.* **214**, 1–12.

Barbosa, C., Peixeiro, I. and Romao, L. (2013) Gene expression regulation by upstream open reading frames and human disease. *PLoS Genet.* **9**, e1003529.

Bembom, O. (2007) Sequence logos for DNA sequence alignments. R package version, 1.

Calvo, S.E., Pagliarini, D.J. and Mootha, V.K. (2009) Upstream open reading frames cause widespread reduction of protein expression and are polymorphic among humans. *Proc. Natl Acad. Sci. U. S. A.* **106**, 7507–7512.

Cattivelli, L., Rizza, F., Badeck, F.W., Mazzucotelli, E., Mastrangelo, A.M., Francia, E., Mare, C., Tondelli, A. and Stanca, A.M. (2008) Drought tolerance improvement in crop plants: an integrated view from breeding to genomics. *Field. Crop. Res.* **105**, 1–14.

Chang, K.S., Lee, S.H., Hwang, S.B. and Park, K.Y. (2000) Characterization and translational regulation of the arginine decarboxylase gene in carnation (Dianthus caryophyllus L.). *Plant J.* **24**, 45–56.

Chew, G.L., Pauli, A., Rinn, J.L., Regev, A., Schier, A.F. and Valen, E. (2013) Ribosome profiling reveals resemblance between long non-coding RNAs and 5′ leaders of coding RNAs. *Development*, **140**, 2828–2834.

Ciais, P., Reichstein, M., Viovy, N. *et al.* (2005) Europe-wide reduction in primary productivity caused by the heat and drought in 2003. *Nature*, **437**, 529–533.

Damiani, R.D. Jr and Wessler, S.R. (1993) An upstream open reading frame represses expression of *Lc,* a member of the *R/B* family of maize transcriptional activators. *Proc. Natl Acad. Sci. U. S. A.* **90**, 8244–8248.

Degenkolbe, T., Do, P.T., Zuther, E., Repsilber, D., Walther, D., Hincha, D.K. and Kohl, K.I. (2009) Expression profiling of rice cultivars differing in their tolerance to long-term drought stress. *Plant Mol. Biol.* **69**, 133–153.

Du, Z., Zhou, X., Ling, Y., Zhang, Z. and Su, Z. (2010) agriGO: a GO analysis toolkit for the agricultural community. *Nucleic Acids Res.* **38**, W64–W70.

Dunn, J.G., Foo, C.K., Belletier, N.G., Gavis, E.R. and Weissman, J.S. (2013) Ribosome profiling reveals pervasive and regulated stop codon readthrough in *Drosophila melanogaster*. *Elife*, **2**, e01179.

Ebina, I., Takemoto-Tsutsumi, M., Watanabe, S. *et al.* (2015) Identification of novel Arabidopsis thaliana upstream open reading frames that control expression of the main coding sequences in a peptide sequence-dependent manner. *Nucleic Acids Res.* **43**, 1562–1576.

Gerashchenko, M.V., Lobanov, A.V. and Gladyshev, V.N. (2012) Genome-wide ribosome profiling reveals complex translational regulation in response to oxidative stress. *Proc. Natl Acad. Sci. U. S. A.* **109**, 17394–17399.

Guo, H., Ingolia, N.T., Weissman, J.S. and Bartel, D.P. (2010) Mammalian microRNAs predominantly act to decrease target mRNA levels. *Nature*, **466**, 835–840.

Harb, A., Krishnan, A., Ambavaram, M.M. and Pereira, A. (2010) Molecular and physiological analysis of drought stress in *Arabidopsis* reveals early responses leading to acclimation in plant growth. *Plant Physiol.*, **154**, 1254–1271.

Hayano-Kanashiro, C., Calderon-Vazquez, C., Ibarra-Laclette, E., Herrera-Estrella, L. and Simpson, J. (2009) Analysis of gene expression and physiological responses in three Mexican maize landraces under drought stress and recovery irrigation. *PLoS ONE*, **4**, e7531.

Hayden, C.A. and Jorgensen, R.A. (2007) Identification of novel conserved peptide uORF homology groups in Arabidopsis and rice reveals ancient eukaryotic origin of select groups and preferential association with transcription factor-encoding genes. *BMC Biol.* **5**, 32.

Hsiao, T.C. (1970) Rapid changes in levels of polyribosomes in *Zea mays* in response to water stress. *Plant Physiol.* **46**, 281–285.

Ingolia, N.T., Ghaemmaghami, S., Newman, J.R. and Weissman, J.S. (2009) Genome-wide analysis *in vivo* of translation with nucleotide resolution using ribosome profiling. *Science*, **324**, 218–223.

Ingolia, N.T., Lareau, L.F. and Weissman, J.S. (2011) Ribosome profiling of mouse embryonic stem cells reveals the complexity and dynamics of mammalian proteomes. *Cell*, **147**, 789–802.

Ingolia, N.T., Brar, G.A., Rouskin, S., McGeachy, A.M. and Weissman, J.S. (2012) The ribosome profiling strategy for monitoring translation *in vivo* by deep sequencing of ribosome-protected mRNA fragments. *Nat. Protoc.* **7**, 1534–1550.

Juntawong, P., Girke, T., Bazin, J. and Bailey-Serres, J. (2014) Translational dynamics revealed by genome-wide profiling of ribosome footprints in *Arabidopsis*. *Proc. Natl Acad. Sci. U. S. A.* **111**, E203–E212.

Kakumanu, A., Ambavaram, M.M., Klumas, C., Krishnan, A., Batlang, U., Myers, E., Grene, R. and Pereira, A. (2012) Effects of drought on gene expression in maize reproductive and leaf meristem tissue revealed by RNA-seq. *Plant Physiol.* **160**, 846–867.

Kawaguchi, R., Williams, A.J., Bray, E.A. and Bailey-Serres, J. (2003) Water-deficit-induced translational control in Nicotiana tabacum. *Plant, Cell Environ.* **26**, 221–229.

Kawaguchi, R., Girke, T., Bray, E.A. and Bailey-Serres, J. (2004) Differential mRNA translation contributes to gene regulation under non-stress and dehydration stress conditions in Arabidopsis thaliana. *Plant J.* **38**, 823–839.

Kozak, M. (1986) Point mutations define a sequence flanking the AUG initiator codon that modulates translation by eukaryotic ribosomes. *Cell*, **44**, 283–292.

Kozak, M. (2002) Pushing the limits of the scanning mechanism for initiation of translation. *Gene*, **299**, 1–34.

Lackner, D.H., Schmidt, M.W., Wu, S., Wolf, D.A. and Bahler, J. (2012) Regulation of transcriptome, translation, and proteome in response to environmental stress in fission yeast. *Genome Biol.* **13**, R25.

Laing, W.A., Martinez-Sanchez, M., Wright, M.A. *et al.* (2015) An upstream open reading frame is essential for feedback regulation of ascorbate biosynthesis in Arabidopsis. *Plant Cell*, **27**, 772–786.

Langmead, B., Trapnell, C., Pop, M. and Salzberg, S.L. (2009) Ultrafast and memory-efficient alignment of short DNA sequences to the human genome. *Genome Biol.* **10**, R25.

Lee, M.V., Topper, S.E., Hubler, S.L., Hose, J., Wenger, C.D., Coon, J.J. and Gasch, A.P. (2011) A dynamic model of proteome changes reveals new roles for transcript alteration in yeast. *Mol. Syst. Biol.* **7**, 514.

Li, P., Ponnala, L., Gandotra, N. *et al.* (2010) The developmental dynamics of the maize leaf transcriptome. *Nat. Genet.* **42**, 1060–1067.

Li, S., Liu, L., Zhuang, X. *et al.* (2013) MicroRNAs inhibit the translation of target mRNAs on the endoplasmic reticulum in *Arabidopsis*. *Cell*, **153**, 562–574.

Liu, M.J., Wu, S.H., Chen, H.M. and Wu, S.H. (2012) Widespread translational control contributes to the regulation of *Arabidopsis* photomorphogenesis. *Mol. Syst. Biol.* **8**, 566.

Liu, M.J., Wu, S.H., Wu, J.F., Lin, W.D., Wu, Y.C., Tsai, T.Y., Tsai, H.L. and Wu, S.H. (2013) Translational landscape of photomorphogenic *Arabidopsis*. *Plant Cell*, **25**, 3699–3710.

Lohmer, S., Maddaloni, M., Motto, M., Salamini, F. and Thompson, R.D. (1993) Translation of the mRNA of the maize transcriptional activator *Opaque-2* is inhibited by upstream open reading frames present in the leader sequence. *Plant Cell*, **5**, 65–73.

Ludwig, S.R., Habera, L.F., Dellaporta, S.L. and Wessler, S.R. (1989) *Lc,* a member of the maize R gene family responsible for tissue-specific anthocyanin production, encodes a protein similar to transcriptional activators and contains the *myc*-homology region. *Proc. Natl Acad. Sci. U. S. A.* **86**, 7092–7096.

Mardanova, E.S., Zamchuk, L.A., Skulachev, M.V. and Ravin, N.V. (2008) The 5′ untranslated region of the maize alcohol dehydrogenase gene contains an internal ribosome entry site. *Gene*, **420**, 11–16.

Michel, A.M., Choudhury, K.R., Firth, A.E., Ingolia, N.T., Atkins, J.F. and Baranov, P.V. (2012) Observation of dually decoded regions of the human genome using ribosome profiling data. *Genome Res.* **22**, 2219–2229.

Morris, D.R. and Geballe, A.P. (2000) Upstream open reading frames as regulators of mRNA translation. *Mol. Cell. Biol.* **20**, 8635–8642.

Mustroph, A., Juntawong, P. and Bailey-Serres, J. (2009) Isolation of plant polysomal mRNA by differential centrifugation and ribosome immunopurification methods. *Methods Mol. Biol.* **553**, 109–126.

Pajerowska-Mukhtar, K.M., Wang, W., Tada, Y., Oka, N., Tucker, C.L., Fonseca, J.P. and Dong, X. (2012) The HSF-like transcription factor TBF1 is a major molecular switch for plant growth-to-defense transition. *Curr. Biol.* **22**, 103–112.

Raymond Hunt, E. Jr, Rock, B.N. and Nobel, P.S. (1987) Measurement of leaf relative water content by infrared reflectance. *Remote Sens. Environ.* **22**, 429–435.

Ringner, M. and Krogh, M. (2005) Folding free energies of 5′-UTRs impact post-transcriptional regulation on a genomic scale in yeast. *PLoS Comput. Biol.* **1**, 582–592.

Rooijers, K., Loayza-Puch, F., Nijtmans, L.G. and Agami, R. (2013) Ribosome profiling reveals features of normal and disease-associated mitochondrial translation. *Nat. Commun.* **4**, 2886.

Sachs, M.S. and Geballe, A.P. (2006) Downstream control of upstream open reading frames. *Genes Dev.* **20**, 915–921.

Schnable, P.S., Ware, D., Fulton, R.S. *et al.* (2009) The B73 maize genome: complexity, diversity, and dynamics. *Science*, **326**, 1112–1115.

Seki, M., Narusaka, M., Ishida, J., Nanjo, T., Fujita, M., Oono, Y., Kamiya, A., Nakajima, M., Enju, A. and Sakurai, T. (2002) Monitoring the expression profiles of 7000 Arabidopsis genes under drought, cold and high-salinity stresses using a full-length cDNA microarray. *Plant J.* **31**, 279–292.

Shalgi, R., Hurt, J.A., Krykbaeva, I., Taipale, M., Lindquist, S. and Burge, C.B. (2013) Widespread regulation of translation by elongation pausing in heat shock. *Mol. Cell*, **49**, 439–452.

Shenton, D., Smirnova, J.B., Selley, J.N., Carroll, K., Hubbard, S.J., Pavitt, G.D., Ashe, M.P. and Grant, C.M. (2006) Global translational responses to oxidative stress impact upon multiple levels of protein synthesis. *J. Biol. Chem.* **281**, 29011–29021.

Shinozaki, K. and Yamaguchi-Shinozaki, K. (2007) Gene networks involved in drought stress response and tolerance. *J. Exp. Bot.* **58**, 221–227.

Sonenberg, N. and Hinnebusch, A.G. (2009) Regulation of translation initiation in eukaryotes: mechanisms and biological targets. *Cell*, **136**, 731–745.

de Sousa Abreu, R., Penalva, L.O., Marcotte, E.M. and Vogel, C. (2009) Global signatures of protein and mRNA expression levels. *Mol. BioSyst.* **5**, 1512–1526.

Spriggs, K.A., Stoneley, M., Bushell, M. and Willis, A.E. (2008) Re-programming of translation following cell stress allows IRES-mediated translation to predominate. *Biol. Cell*, **100**, 27–38.

Spriggs, K.A., Bushell, M. and Willis, A.E. (2010) Translational regulation of gene expression during conditions of cell stress. *Mol. Cell*, **40**, 228–237.

Trapnell, C., Pachter, L. and Salzberg, S.L. (2009) TopHat: discovering splice junctions with RNA-seq. *Bioinformatics*, **25**, 1105–1111.

Tuller, T., Carmi, A., Vestsigian, K., Navon, S., Dorfan, Y., Zaborske, J., Pan, T., Dahan, O., Furman, I. and Pilpel, Y. (2010) An evolutionarily conserved mechanism for controlling the efficiency of protein translation. *Cell*, **141**, 344–354.

Uchiyama-Kadokura, N., Murakami, K., Takemoto, M., Koyanagi, N., Murota, K., Naito, S. and Onouchi, H. (2014) Polyamine-responsive ribosomal arrest at the stop codon of an upstream open reading frame of the AdoMetDC1 gene triggers nonsense-mediated mRNA decay in Arabidopsis thaliana. *Plant Cell Physiol.* **55**, 1556–1567.

Vogel, C., Abreu Rde, S., Ko, D., Le, S.Y., Shapiro, B.A., Burns, S.C., Sandhu, D., Boutz, D.R., Marcotte, E.M. and Penalva, L.O. (2010) Sequence signatures and mRNA concentration can explain two-thirds of protein abundance variation in a human cell line. *Mol. Syst. Biol.* **6**, 400.

Wang, L. and Roossinck, M.J. (2006) Comparative analysis of expressed sequences reveals a conserved pattern of optimal codon usage in plants. *Plant Mol. Biol.* **61**, 699–710.

Wang, L. and Wessler, S.R. (1998) Inefficient reinitiation is responsible for upstream open reading frame–mediated translational repression of the maize *R* gene. *Plant Cell*, **10**, 1733–1745.

Wang, L. and Wessler, S. (2001) Role of mRNA secondary structure in translational repression of the maize transcriptional activator *Lc*. *Plant Physiol.* **125**, 1380–1387.

Wang, Z., Gerstein, M. and Snyder, M. (2009) RNA-Seq: a revolutionary tool for transcriptomics. *Nat. Rev. Genet.* **10**, 57–63.

Wiese, A., Elzinga, N., Wobbes, B. and Smeekens, S. (2004) A conserved upstream open reading frame mediates sucrose-induced repression of translation. *Plant Cell*, **16**, 1717–1729.

Young, D.J., Guydosh, N.R., Zhang, F., Hinnebusch, A.G. and Green, R. (2015) Rli1/ABCE1 Recycles Terminating Ribosomes and Controls Translation Reinitiation in 3′UTRs *In Vivo*. *Cell*, **162**, 872–884.

Zoschke, R., Watkins, K.P. and Barkan, A. (2013) A rapid ribosome profiling method elucidates chloroplast ribosome behavior *in vivo*. *Plant Cell*, **25**, 2265–2275.